

# Constraints on the $\Lambda$ CDM model with redshift tomography

Rong-Gen Cai<sup>1,\*</sup> Zong-Kuan Guo<sup>1,†</sup> and Bo Tang<sup>1‡</sup>

<sup>1</sup> *State Key Laboratory of Theoretical Physics,  
Institute of Theoretical Physics,  
Chinese Academy of Sciences,  
P.O. Box 2735, Beijing 100190, China.*

(Dated: November 16, 2018)

## Abstract

Recently released Planck data favor a lower value of the Hubble constant and a higher value of the fraction matter density in the standard  $\Lambda$ CDM model, which are discrepant with some of the low-redshift measurements. Within the context of this cosmology, we examine the consistency of the estimated values for the Hubble constant and fraction matter density with redshift tomography. Using the SNe Ia, Hubble parameter, BAO and reduced CMB data, which are divided into three bins, we find no statistical evidence for any tension in the three redshift bins.

---

\*Electronic address: cairg@itp.ac.cn

†Electronic address: guozk@itp.ac.cn

‡Electronic address: tangbo@itp.ac.cn

## I. INTRODUCTION

More than one decade ago it was found that our universe is in an accelerating expansion based on the distance measurement of type Ia supernovae (SNe Ia) [1, 2]. This observation is consistent with other astronomical observations such as Hubble parameter, large scale structure and cosmic microwave background radiation (CMB), etc. To explain this accelerating expansion, one has to introduce the so-called dark energy with negative pressure in the general relativity framework, or to modify the general relativity at cosmic scales. Although suffered from some theoretical issues, the cosmological constant [3, 4] introduced by Einstein himself in 1917 is the most simple and economical candidate for the dark energy. Indeed the standard  $\Lambda$ CDM model turns out to be consistent with several precise astronomical observations, such as SNe Ia [5], Wilkinson Microwave Anisotropy Probe (WMAP) measurements of CMB [6], and baryon acoustic oscillation, etc. If the standard  $\Lambda$ CDM model properly describes our universe, the current Hubble constant  $H_0$  and fraction matter density  $\Omega_{m0}$  should be consistent with those estimated by different observations made at different redshifts.

However, the recently released Planck data [7] favor a higher value of  $\Omega_{m0} = 0.315 \pm 0.017$  and a lower value of  $H_0 = (67.3 \pm 1.2) \text{ km s}^{-1} \text{ Mpc}^{-1}$  in the standard six-parameter  $\Lambda$ CDM cosmology, obtained by using Planck+WP, where WP stands for WMAP polarization data. These values are in tension with the magnitude-redshift relation for SNe Ia and recent direct measurements of  $H_0$ , such as the Hubble space telescope observations of Cepheid variables with  $H_0 = (73.8 \pm 2.4) \text{ km s}^{-1} \text{ Mpc}^{-1}$  [8] and  $H_0 = [74.3 \pm 1.5(\text{stat.}) \pm 2.1(\text{sys.})] \text{ km s}^{-1} \text{ Mpc}^{-1}$  obtained by using a mid-infrared calibration of the Cepheid distance scale based on observations at  $3.6 \mu\text{m}$  with the Spitzer Space Telescope [9]. Of course, if relax the restriction of the standard six-parameter  $\Lambda$ CDM model, for example, consider the dynamical dark energy model [10] or include the dark radiation [11], the tension might be alleviated. In [12], Hu *et al.* found that there is another way to alleviate this tension in modified gravity models. Furthermore it was reported in [13] that this tension may also be alleviated by if one first calibrates the light-curve fitting parameters in the distance estimation in SNe Ia observations with the angular diameter distance data of the galaxy clusters, with the help of the distance-duality relation. Very recently, Efstathiou [14] reanalyzed the Cepheid data and found  $H_0 = (70.6 \pm 3.3) \text{ km s}^{-1} \text{ Mpc}^{-1}$  based on the NGC 4258 maser distance and

$H_0 = (72.5 \pm 2.5) \text{ km s}^{-1} \text{ Mpc}^{-1}$  with three distance anchors combined, which alleviates the tension compared to the result obtained by Riess *et al.* [8], but the latter still differs by  $1.9\sigma$  from the Planck value. In addition, by comparing the eight ultra low redshift SNe Ia data ( $z = 0.0043$  to  $0.0072$ ) [8], with low redshift data ( $z < 0.04$ ) from the Union2.1 compilation [15] and Planck data [7], Zhang and Ma found that the present expansion of the universe estimated from the low redshift measurements is higher than the one estimated from high redshift observations in the  $\Lambda$ CDM model [16]. In other words, higher redshift measurements give a lower value of  $h$ , the reduced Hubble constant.

These discrepancies seemingly imply that the standard  $\Lambda$ CDM model cannot well describe the properties of the universe at all redshift if the major sources of systematic errors of these observations have been controlled. In this paper we detect these discrepancies in the  $\Lambda$ CDM model with redshift tomography. We divide the redshift range under consideration into three bins and use observation data in each bin to separately constrain the Hubble constant and fraction matter density in the  $\Lambda$ CDM model. In the literature the redshift tomography is often used to see the dynamical property of dark energy by piecewise parametrization of the equation of state of the dark energy. Here our goal is to see the consistency of the  $\Lambda$ CDM model at different redshifts, therefore we focus on the  $\Lambda$ CDM model. The data sets we use here include the Union2.1 SNe Ia data [15], 19 Hubble parameter  $H(z)$  data [17–19], Baryon Acoustic Oscillation (BAO) data measured by the 6 degree Field Galaxy Survey (6dFGS), SDSS DR7, SDSS DR9 and WiggleZ surveys, reduced nine-year WMAP data (WMAP9) and reduced Planck data both based on the flat  $\Lambda$ CDM model.

The paper is organized as follows. In section II we describe the redshift tomography method and observational data. In section III we show the results of different combination of data sets to constrain the base  $\Lambda$ CDM model based on the SNe Ia data and the redshift tomography analysis. The results are summarized in section IV.

## II. METHOD AND DATA

In a spatially flat Friedmann-Robertson-Walker universe, the Hubble parameter is given by the Friedmann equation

$$H^2(z) = H_0^2 \left[ \Omega_{r0}(1+z)^4 + \Omega_{dm0}(1+z)^3 + \Omega_{b0}(1+z)^3 + (1 - \Omega_{m0} - \Omega_{r0}) \right], \quad (1)$$

for the  $\Lambda$ CDM model, where the redshift  $z$  is defined by  $(1+z) = 1/a$ , and  $\Omega_{r0}$ ,  $\Omega_{dm0}$  and  $\Omega_{b0}$  are the present values of the fraction energy density for radiation, dark matter and baryon matter, respectively. The latter two are often written as the total matter density  $\Omega_{m0} = \Omega_{b0} + \Omega_{dm0}$ . The radiation density is the sum of photons and relativistic neutrinos [6]:

$$\Omega_{r0} = \Omega_{\gamma}^{(0)}(1 + 0.2271N_{eff}), \quad (2)$$

where  $N_{eff} = 3.046$  is the effective number of neutrino species in the Standard Model [20], and  $\Omega_{\gamma}^{(0)} = 2.469 \times 10^{-5}h^{-2}$  for  $T_{\text{CMB}} = 2.725K$  ( $h \equiv H_0/100 \text{ km s}^{-1} \text{ Mpc}^{-1}$ ).

We focus on constraints on the Hubble constant and the fraction matter density in the context of the  $\Lambda$ CDM cosmology from the low-redshift observational data including Union2.1 SNe Ia sample, Hubble parameter and BAO data, in combination with the high-redshift CMB measurements. We adopt a redshift tomography method to examine the flat  $\Lambda$ CDM model. Since the SNe Ia data cannot alone constrain the  $\Lambda$ CDM model very well, it could be even worse in each redshift bin because of the decreasing of data points (so do the Hubble parameters), we then divide the redshift into three bins so that the BAO data can distribute uniformly in the first two bins, while the CMB data are in the third bin. As a result, these data are divided into three combinations in the following redshift bins:  $0 - 0.28$ ,  $0.28 - 0.73$  and  $> 0.73$ . The distribution of data is listed in Table 1. To see the difference, we will use WMAP9 and Planck data separately.

redshift bin	SNe Ia	Hubble	BAO	CMB
$0 - 0.28$	283	5	6dF, DR7a, RBAO1	–
$0.28 - 0.73$	212	5	DR7-re, WiggleZ, DR9, RBAO2	–
$> 0.73$	85	9	–	WMAP9/Planck

Table 1: Distribution of SNe Ia, Hubble, BAO, CMB data in three redshift bins.

The best-fit values of  $\Omega_{m0}$  and  $h$ , and their 68% and 95% confidence level (CL) errors are obtained by performing the Markov Chain Monte Carlo analysis in the multidimensional parameter space in a Bayesian framework. Since the Hubble constant is completely degenerate with the absolute magnitude of SNe Ia, SNe Ia data are not sensitive to the Hubble constant. Therefore, in our analysis we marginalize analytically over the Hubble constant when the SNe Ia data are concerned. Moreover, note that the fraction baryon energy density  $\Omega_{b0}$  is involved in the likelihood for the BAO and CMB data.

## A. Type Ia Supernovae

The SNe Ia data set is an important tool to understand the evolution of the universe. In this work, we adopt the Union2.1 compilation [15], containing 580 SNe Ia data over the redshift range  $0.015 \leq z \leq 1.414$ . The chisquare is defined as as

$$\chi_{SN}^2 = \sum_{i=1}^N \frac{[\mu^{obs}(z_i) - \mu^{th}(z_i)]^2}{\sigma_{SN}^2(z_i)}, \quad (3)$$

where  $N$  is the data number in the redshift interval we are interested in,  $\mu^{obs}(z)$  is the measured distance modulus from the data and  $\mu^{th}(z)$  is the theoretical distance modulus, defined as

$$\mu^{th}(z) = 5 \log_{10} d_L + \mu_0, \quad \mu_0 = 42.384 - 5 \log_{10} h. \quad (4)$$

The luminosity distance is

$$d_L(z) = (1+z) \int_0^z \frac{dx}{E(x)}, \quad (5)$$

where  $E(z) \equiv H(z)/H_0$ . We can eliminate the nuisance parameter  $\mu_0$  by expanding  $\chi^2$  with respect to  $\mu_0$  [21] :

$$\chi_{SN}^2 = A + 2B\mu_0 + C\mu_0^2, \quad (6)$$

where

$$\begin{aligned} A &= \sum_{i=1}^N \frac{[\mu^{th}(z_i; \mu_0 = 0) - \mu^{obs}(z_i)]^2}{\sigma_{SN}^2(z_i)}, \\ B &= \sum_{i=1}^N \frac{\mu^{th}(z_i; \mu_0 = 0) - \mu^{obs}(z_i)}{\sigma_{SN}^2(z_i)}, \\ C &= \sum_{i=1}^N \frac{1}{\sigma_{SN}^2(z_i)}. \end{aligned} \quad (7)$$

The  $\chi_{SN}^2$  has a minimum as

$$\tilde{\chi}_{SN}^2 = A - B^2/C, \quad (8)$$

which is independent of  $\mu_0$ . This technique is equivalent to performing a uniform marginalization over  $\mu_0$  [21]. We will adopt  $\tilde{\chi}_{SN}^2$  as the goodness of fitting instead of  $\chi_{SN}^2$ .

## B. Observational Hubble parameter (HUB)

The observational Hubble parameter can be obtained by using the differential ages of passively evolving galaxies as

$$H = -\frac{1}{1+z} \frac{\Delta z}{\Delta t}. \quad (9)$$

We use 19 observational Hubble data over the redshift range  $0.07 \leq z \leq 2.3$ , which contain 11 observational Hubble data obtained from the differential ages of passively evolving galaxies [17, 18], and 8  $H(z)$  data at eight different redshifts obtained from the differential spectroscopic evolution of early type galaxies as a function of redshift [19]. The chisquare is defined as

$$\chi_{HUB}^2 = \sum_{i=1}^N \frac{[H_{th}(z_i) - H_{obs}(z_i)]^2}{\sigma_H^2(z_i)}, \quad (10)$$

where  $H_{th}(z)$  and  $H_{obs}(z)$  are the theoretical and observed values of Hubble parameter, and  $\sigma_H$  denotes the error bar of observed data.

## C. Baryon Acoustic Oscillation

As a ruler to measure the distance-redshift relation, Baryon Acoustic Oscillation provides an efficient method for measuring the expansion history of the universe by using features in the cluster of galaxies with large scale surveys. Here we use the results from the following five BAO surveys: the 6dF Galaxy Survey, SDSS DR7, SDSS DR9, WiggleZ measurements and the radial BAO measurement.

### 1. 6dF Galaxy Survey

The 6dFGS BAO detection allows us to constrain the distance-redshift relation at  $z_{eff} = 0.106$  [22]. The low effective redshift of 6dFGS makes it a competitive and independent alternative to Cepheids and low redshift supernovae in constraining the Hubble constant. They achieved a measurement of the distance ratio

$$\frac{r_s(z_d)}{D_V(z = 0.106)} = 0.336 \pm 0.015, \quad (11)$$

where  $r_s(z_d)$  is the comoving sound horizon at the baryon drag epoch when baryons became dynamically decoupled from photons. The redshift  $z_d$  is well approximated by [23]

$$z_d = \frac{1291(\Omega_{m0}h^2)^{0.251}}{1 + 0.659(\Omega_{m0}h^2)^{0.828}}[1 + b_1(\Omega_{b0}h^2)^{b_2}], \quad (12)$$

where

$$\begin{aligned} b_1 &= 0.313(\Omega_{m0}h^2)^{-0.419}[1 + 0.607(\Omega_{m0}h^2)^{0.674}], \\ b_2 &= 0.238(\Omega_{m0}h^2)^{0.223}. \end{aligned} \quad (13)$$

The effective ‘‘volume’’ distance  $D_V$  is a combination of the angular-diameter distance  $D_A(z)$  and the Hubble parameter  $H(z)$ ,

$$\begin{aligned} D_V(z) &= \left[ \left( \int_0^z \frac{dx}{H(x)} \right)^2 \frac{z}{H(z)} \right]^{1/3} \\ &= [(1+z)^2 D_A(z)^2 \frac{z}{H(z)}]^{1/3}. \end{aligned} \quad (14)$$

The  $\chi_{6dF}^2$  is given by

$$\chi_{6dF}^2 = \frac{[(r_s(z_d)/D_V(0.106))_{th} - 0.336]^2}{0.015^2}. \quad (15)$$

## 2. SDSS DR7

The joint analysis of the 2-degree Field Galaxy Redshift Survey data and the Sloan Digital Sky Survey Data Release 7 data gives the distance ratio at  $z = 0.2$  and  $z = 0.35$  [24]:

$$\begin{aligned} \frac{r_s(z_d)}{D_V(z = 0.2)} &= 0.1905 \pm 0.0061, \\ \frac{r_s(z_d)}{D_V(z = 0.35)} &= 0.1097 \pm 0.0036. \end{aligned} \quad (16)$$

When the two data points are in the same redshift bin, we adopt the  $\chi_{DR7}^2$  given by

$$\chi_{DR7}^2 = X^T V^{-1} X, \quad (17)$$

where

$$X = \begin{bmatrix} \left[ \frac{r_s(z_d)}{D_V(0.2)} \right]_{th} - 0.1905 \\ \left[ \frac{r_s(z_d)}{D_V(0.35)} \right]_{th} - 0.1097 \end{bmatrix}, \quad (18)$$

and the inverse covariance matrix is

$$V^{-1} = \begin{bmatrix} 30124.1 & -17226.9 \\ -17226.9 & 86976.6 \end{bmatrix}. \quad (19)$$

On the other hand, when the two data points are in the different redshift bin, their  $\chi_{DR7}^2$  are respectively given by

$$\begin{aligned}\chi_{DR7a}^2 &= \frac{[(\frac{r_s(z_d)}{D_V(0.2)})_{th} - 0.1905]^2}{0.0061^2}, \\ \chi_{DR7b}^2 &= \frac{[(\frac{r_s(z_d)}{D_V(0.35)})_{th} - 0.1097]^2}{0.0036^2}.\end{aligned}\tag{20}$$

### 3. SDSS DR7 reanalysis

By applying the reconstruction technique [25] to the clustering of galaxies from the SDSS DR7 Luminous Red Galaxies sample, and sharpening the BAO feature, Padmanabhan *et al.* obtained the distance ratio at  $z = 0.35$  [26] :

$$\frac{r_s(z_d)}{D_V(z = 0.35)} = 0.1126 \pm 0.0022.\tag{21}$$

The  $\chi_{DR7-re}^2$  used in the Markov Chain Monte Carlo analysis is

$$\chi_{DR7re}^2 = \frac{[(\frac{r_s(z_d)}{D_V(0.35)})_{th} - 0.1126]^2}{0.0022^2}.\tag{22}$$

Since the SDSS DR7 and SDSS DR7 reanalysis results are based on the same survey and the latter gives a higher precision than the former, we include the SDSS DR7 reanalysis data when we do the whole redshift analysis but not both together. On the other hand, when we do redshift tomography, we may refer to part of the SDSS DR7 data at  $z = 0.2$  and when the redshift bin contains  $z = 0.35$ , we will use the SDSS DR7 reanalysis data.

### 4. SDSS DR9

The SDSS DR9 measurement at  $z = 0.57$  analyzed by Anderson *et al.* [27] gives

$$\frac{r_s(z_d)}{D_V(z = 0.57)} = 0.0732 \pm 0.0012,\tag{23}$$

which is the most precise determination of the acoustic oscillation scale to date. The chisquare is defined as

$$\chi_{DR9}^2 = \frac{[(\frac{r_s(z_d)}{D_V(0.57)})_{th} - 0.0732]^2}{0.0012^2}.\tag{24}$$

### 5. The WiggleZ measurements

The WiggleZ team encodes some shape information on the power spectrum to measure the acoustic parameter [28]:

$$A(z) = \frac{D_V(z)\sqrt{\Omega_{m0}H_0}}{z}. \quad (25)$$

The measurements of the baryon acoustic peak at redshifts  $z = 0.44, 0.6$  and  $0.73$  in the galaxy correlation function of the final dataset of the WiggleZ Dark Energy Survey give the acoustic parameter:

$$\begin{aligned} A(z = 0.44) &= 0.474 \pm 0.034, \\ A(z = 0.60) &= 0.442 \pm 0.020, \\ A(z = 0.73) &= 0.424 \pm 0.021. \end{aligned} \quad (26)$$

The chisquare is defined as

$$\chi_{Wig}^2 = X^T V^{-1} X, \quad (27)$$

where

$$X = \begin{bmatrix} A(z = 0.44)_{th} - 0.474 \\ A(z = 0.60)_{th} - 0.442 \\ A(z = 0.73)_{th} - 0.424 \end{bmatrix}, \quad (28)$$

and its inverse covariance matrix is

$$V^{-1} = \begin{bmatrix} 1040.3 & -807.5 & 336.8 \\ -807.5 & 3720.3 & -1551.9 \\ 336.8 & -1551.9 & 2914.9 \end{bmatrix}. \quad (29)$$

### 6. Radial BAO

The radial (line-of-sight) baryon acoustic scale can also be measured by using the SDSS data. It is independent from the BAO measurements described above, which are averaged over all directions or in the transverse directions. The measured quantity is

$$\Delta_z(z) = H(z)r_s(z_d), \quad (30)$$

whose values are given by [29]

$$\begin{aligned} \Delta_z(0.24) &= 0.0407 \pm 0.0011, \\ \Delta_z(0.43) &= 0.0442 \pm 0.0015. \end{aligned} \quad (31)$$

## D. Cosmic Microwave Background

In the CMB measurement, the distance to the last scattering surface can be accurately determined from the locations of peaks and troughs of acoustic oscillations. There are two quantities: one is the “acoustic scale”

$$l_A = (1 + z_*) \frac{\pi D_A(z_*)}{r_s(z_*)}, \quad (32)$$

and the other is the “shift parameter”

$$R = \sqrt{\Omega_{m0} H_0^2} (1 + z_*) D_A(z_*). \quad (33)$$

These quantities can be used to constrain cosmological parameters without need to use the full data of WMAP9 [6]. Here  $z_*$  is the redshift at the last scattering surface [30]

$$z_* = 1048[1 + 0.00124(\Omega_{b0}h^2)^{-0.738}][1 + g_1(\Omega_{m0}h^2)^{g_2}], \quad (34)$$

where

$$\begin{aligned} g_1 &= \frac{0.0783(\Omega_{b0}h^2)^{-0.238}}{1 + 39.5(\Omega_{b0}h^2)^{0.763}}, \\ g_2 &= \frac{0.560}{1 + 21.1(\Omega_{b0}h^2)^{1.81}}. \end{aligned} \quad (35)$$

Wang and Wang [31] have obtained the mean values and covariance matrix of  $\{R, l_A, \Omega_{b0}h^2, n_s\}$  from WMAP9 and Planck data respectively, based on the  $\Lambda$ CDM model without assuming a flat universe. On the other hand, Shafer and Huterer [32] derived the related results about  $\{R, l_A, z_*\}$  from WMAP9 and Planck data respectively, based on the flat  $w$ CDM model. For our propose, following [31] and [32], we first extract the mean values and covariance matrix of  $\{R, l_A, z_*\}$  from WMAP9 and Planck data respectively based on a flat  $\Lambda$ CDM model.

### 1. WMAP9

By using the WMAP9 data, we obtain the mean values for  $\{R, l_A, z_*\}$  as

$$\langle l_A \rangle = 301.95, \quad \langle R \rangle = 1.7257, \quad \langle z_* \rangle = 1088.96. \quad (36)$$

Their inverse covariance matrix is

$$C_{WMAP9}^{-1} = \begin{bmatrix} 3.087 & 15.160 & -1.456 \\ 15.160 & 12805.3 & -217.021 \\ -1.456 & -217.021 & 5.552 \end{bmatrix}. \quad (37)$$

The chisquare for the reduced WMAP9 data is defined by

$$\chi_{WMAP9}^2 = X^T C_{WMAP9}^{-1} X, \quad (38)$$

where

$$X = \begin{bmatrix} l_A - 301.95 \\ R - 1.7257 \\ z_* - 1088.96. \end{bmatrix} \quad (39)$$

## 2. Planck

By using the Planck data, we obtain the mean values for  $\{R, l_A, z_*\}$  as

$$\langle l_A \rangle = 301.65, \quad \langle R \rangle = 1.7500, \quad \langle z_* \rangle = 1090.33. \quad (40)$$

Their inverse covariance matrix is

$$C_{Planck}^{-1} = \begin{bmatrix} 40.909 & -405.455 & -0.5443 \\ -405.455 & 55662.8 & -751.123 \\ -0.5443 & -751.123 & 14.6187 \end{bmatrix}. \quad (41)$$

The chisquare for the reduced Planck data is defined as

$$\chi_{Planck}^2 = X^T C_{Planck}^{-1} X, \quad (42)$$

where

$$X = \begin{bmatrix} l_A - 301.65 \\ R - 1.7500 \\ z_* - 1090.33. \end{bmatrix} \quad (43)$$

## III. RESULTS

Using the Union2.1 sample in combination with other measurements described in the previous section, we give the constraints on the base  $\Lambda$ CDM model. The best-fit values of

$\Omega_{m0}$  and  $h$  with 68% CL errors are summarized in Table 2, and their likelihoods are shown in Figure 1.

From Table 2 we can see that the SNe Ia data alone favor a lower value of  $\Omega_{m0}$  than the SNe Ia data in combination with other datasets. Including the BAO and WMAP9/Planck data improves significantly the constraint on  $\Omega_{m0}$ . Including the reduced Planck data gives the highest  $\Omega_{m0}$  and the lowest  $h$ . We find these estimates of  $\Omega_{m0}$  are consistent with each other within  $1\sigma$  CL, but are in tension with the results derived by Planck [7]. The estimates of  $h$  from the HUB, BAO and WMAP9 are compatible with those from Planck, but are discrepant with those from fitting the calibrated SNe magnitude-redshift relation [8].

data	$\Omega_{m0}$	$h$
<i>SN</i>	$0.2776^{+0.0299}_{-0.0304}$	—
<i>SN + HUB</i>	$0.2834^{+0.0231}_{-0.0227}$	$0.7055^{+0.0234}_{-0.0248}$
<i>SN + HUB + BAO</i>	$0.2875^{+0.0192}_{-0.0192}$	$0.7037^{+0.0241}_{-0.0248}$
<i>SN + BAO + WMAP9</i>	$0.2867^{+0.0113}_{-0.0111}$	$0.7032^{+0.0107}_{-0.0108}$
<i>SN + HUB + BAO + WMAP9</i>	$0.2877^{+0.0111}_{-0.0110}$	$0.7022^{+0.0110}_{-0.0095}$
<i>SN + HUB + BAO + Planck</i>	$0.2969^{+0.0103}_{-0.0086}$	$0.6974^{+0.0082}_{-0.0086}$

Table 2: Constraints with  $1\sigma$  errors on  $\Omega_{m0}$  and  $h$  for the base  $\Lambda$ CDM cosmology from SNe Ia data in combination with HUB, BAO, WMAP9 and Planck.

Using the SN+HUB+BAO+WMAP9/Planck data distributed in three different redshift bins, we present the constraints on  $\Omega_{m0}$  and  $h$  for the  $\Lambda$ CDM model in Table 3. The corresponding marginalized posterior distributions are shown in Figure 2.

Our analysis shows that low-redshift observations give a higher value of  $\Omega_{m0}$ , while high-redshift observations give a lower one by using the SN+HUB+BAO+WMAP9 data. However, the high redshift  $z > 0.73$  observations with Planck data favor a relatively higher value of  $\Omega_{m0}$ , which is inconsistent with the high-redshift value from WMAP9 at about  $1.1\sigma$  CL.

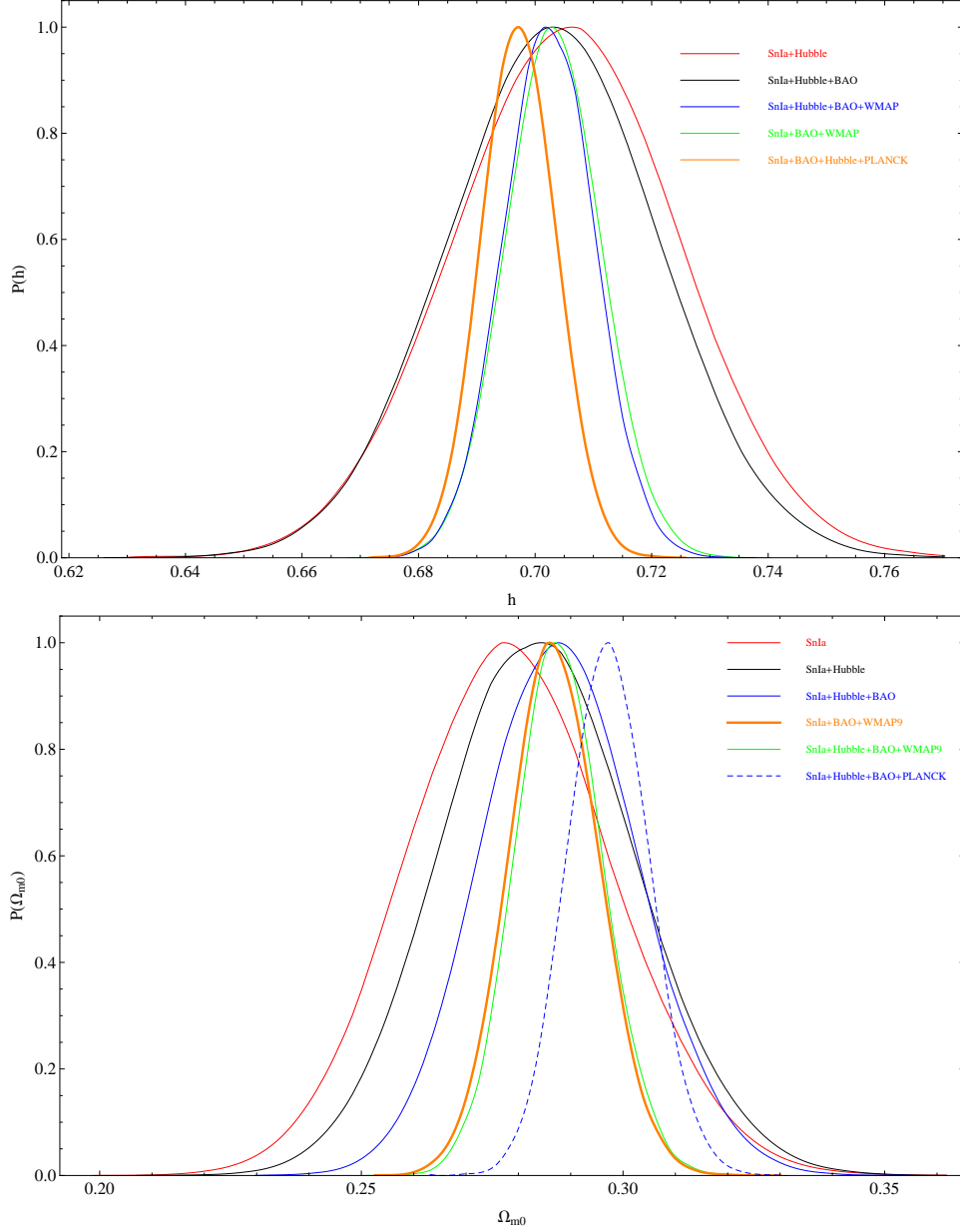


Fig. 1: Marginalized posterior distributions for  $\Omega_{m0}$  (upper) and  $h$  (bottom) from SNe Ia data in combination with HUB, BAO WMAP9 and Planck.

In addition, there are large uncertainties in the estimation of  $\Omega_{m0}$  from the data in the redshift range  $0 < z < 0.28$ . From Table 3 we find that the data in the mid-redshift range  $0.28 < z < 0.73$  favor a lower Hubble constant with a little large uncertainty than the data at low and high redshifts. Figure 3 shows the best-fit values of  $\Omega_{m0}$  and  $h$  with  $1\sigma$  errors for the data in three different redshift bins.

redshift range	$\Omega_{m0}$	$h$
0 – 0.28	$0.3187^{+0.0787}_{-0.0932}$	$0.6870^{+0.0381}_{-0.0298}$
0.28 – 0.73	$0.3032^{+0.0332}_{-0.0327}$	$0.6677^{+0.0556}_{-0.0469}$
> 0.73( <i>WMAP</i> )	$0.2767^{+0.0366}_{-0.0328}$	$0.7123^{+0.0319}_{-0.0345}$
> 0.73( <i>Planck</i> )	$0.3158^{+0.0230}_{-0.0218}$	$0.6831^{+0.0146}_{-0.0181}$
whole( <i>WMAP</i> )	$0.2877^{+0.0111}_{-0.0110}$	$0.7022^{+0.0110}_{-0.0095}$
whole( <i>Planck</i> )	$0.2969^{+0.0103}_{-0.0086}$	$0.6974^{+0.0082}_{-0.0086}$

Table 3: Constraints with  $1\sigma$  errors on  $\Omega_{m0}$  and  $h$  for the base  $\Lambda$ CDM cosmology in three redshift bins from the SN+HUB+BAO+WMAP9 and SN+HUB+BAO+Planck. For a comparison, we also list the constraints in the whole redshift range.

In our analysis the Hubble constant is marginalized as a nuisance parameter in the SNe Ia likelihood function. Therefore, the constraints on  $h$  mainly come from the HUB, BAO and WMAP9/Planck data. In Ref. [16] a higher value of Hubble constant is recently obtained from measurements of nearby SNe Ia with help of measurements of Cepheid variables, than that obtained by Planck. However, our estimates of  $h$  from the data in the redshift ranges of  $z < 0.28$  and  $0.28 < z < 0.73$  are lower than the result obtained in [16]. Moreover, the high-redshift data ( $z > 0.73$ ) including the WMAP9 data favor a higher value of  $h$  than the data in the first two redshift bins.

#### IV. CONCLUSIONS

The estimates of  $\Omega_{m0}$  and  $h$  in the base  $\Lambda$ CDM model should be consistent with each other from measurements made in different redshift intervals, if the simplest  $\Lambda$ CDM model completely describes the evolution of our universe and the unknown sources of systematic errors of these measurements can be negligible. The recent Planck observations of the CMB lead to a Hubble constant of  $h = 0.673 \pm 0.012$  and a matter density parameter of  $\Omega_{m0} = 0.315 \pm 0.017$  [7], which, however, are different from the low- $z$  measurements. In this work, we have studied the consistency of the estimated values for the Hubble constant and matter density parameter from different redshift data.

We have first obtained reduced CMB data for  $\{R, l_A, z_*\}$  from WMAP9 and Planck data,

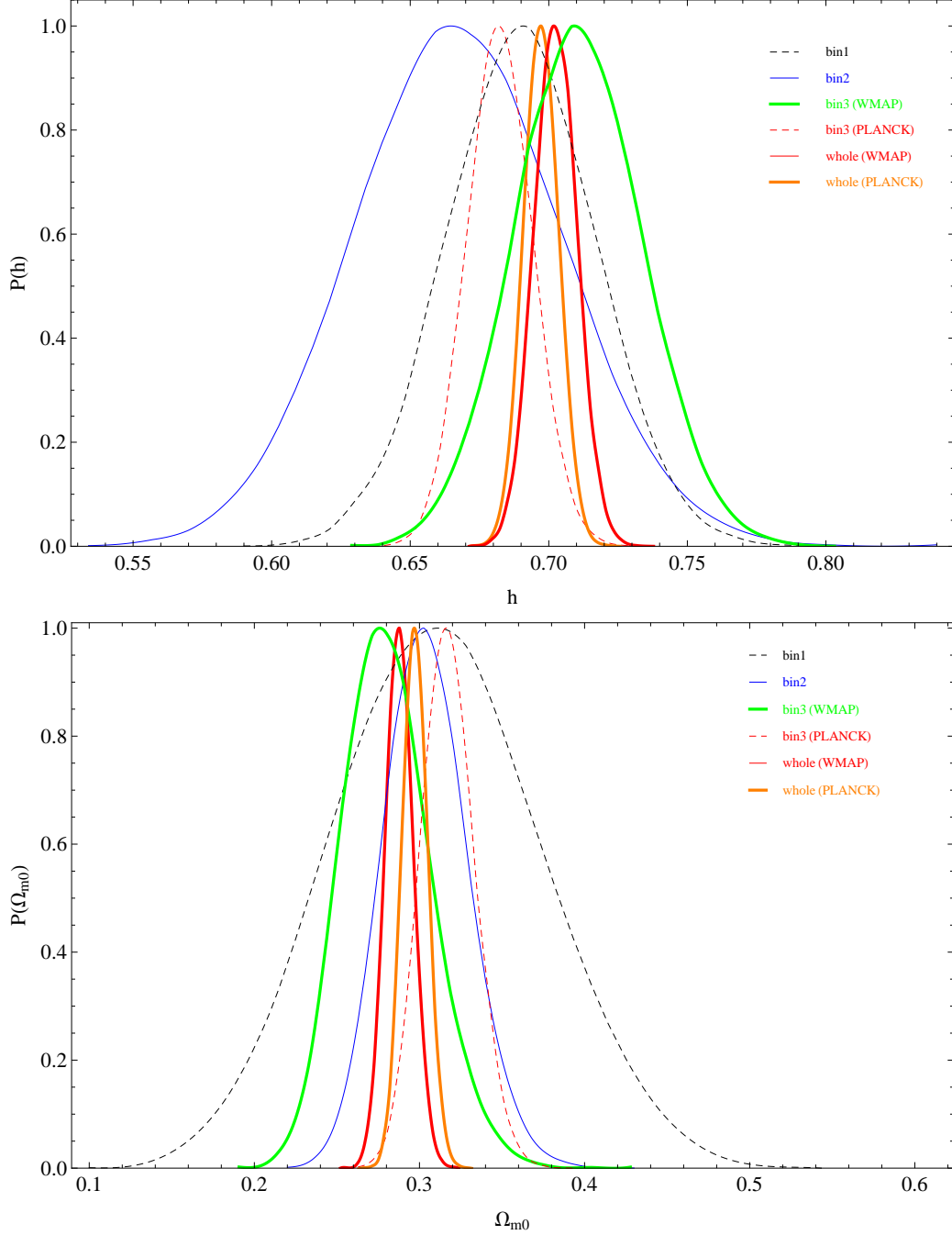


Fig. 2: Marginalized posterior distributions of  $\Omega_{m0}$  (upper) and  $h$  (bottom) for three redshift bins of the SN+HUB+BAO+WMAP9/Planck data.

based on a flat  $\Lambda$ CDM model. We then have placed constraints on the base  $\Lambda$ CDM model using astrophysical measurements of SNe Ia, Hubble and BAO, in combination with the reduced WMAP9/Planck CMB data. We have found that the SNe Ia data alone favor a lower value of  $\Omega_{m0}$  and adding the HUB, BAO, and the reduced WMAP9/reduced Planck

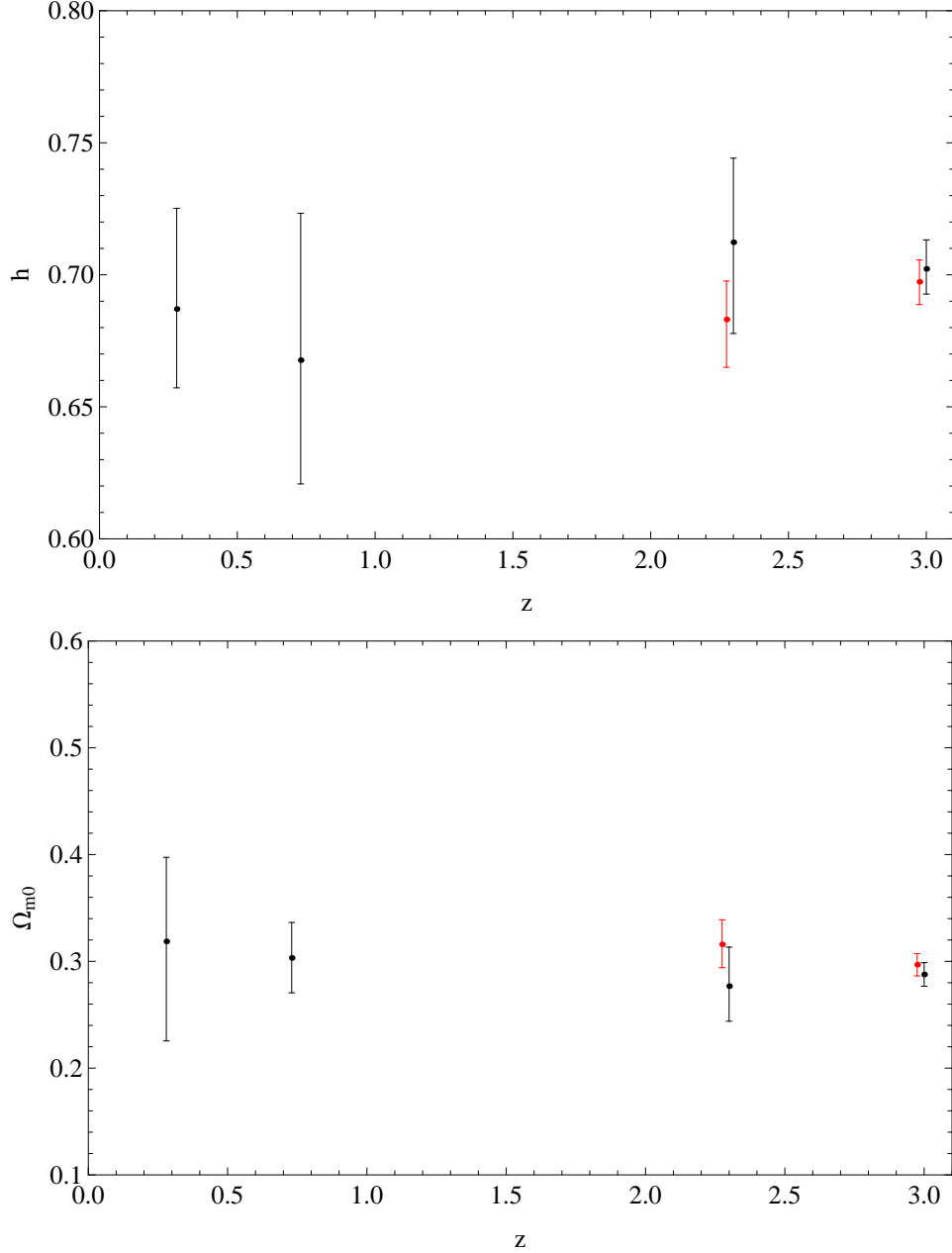


Fig. 3: Best-fit values of  $\Omega_{m0}$  (upper) and  $h$  (bottom) with  $1\sigma$  errors in three redshift bins and in the whole redshift range. The third and fourth error bars in black represent the case containing WMAP9 data, while the red ones represent the case containing Planck data.

data can give a higher one, but it is still in tension with the result reported by Planck. Moreover, the estimates of  $h$  from the HUB, BAO and WMAP9 are compatible with those from Planck, but are discrepant with those from fitting the calibrated SNe magnitude-redshift relation [8]. There is no any tension on  $h$  among three redshift bins, as shown in

Fig. 3.

We have also implemented the redshift tomography analysis in the context of the  $\Lambda$ CDM cosmology with the SNe Ia, HUB, BAO and CMB data. We have found that low-redshift observations ( $z < 0.28$ ) give a higher value of  $\Omega_{m0}$ , as estimated by Planck, while high-redshift observations ( $z > 0.73$ ) with the WMAP9 data give a lower one, which is inconsistent with that from the SN+HUB+BAO data in the high-redshift range in combination with the Planck data at about  $1.1\sigma$  *CL*. In addition, the data in the mid-redshift range  $0.28 < z < 0.73$  favor a lower Hubble constant. The current data cannot provide statistically significant evidence for any tension among the different redshift bins.

### Acknowledgments

This work was supported in part by the National Natural Science Foundation of China (No.10821504, No.10975168, No.11035008 and No.11175225), and in part by the Ministry of Science and Technology of China under Grant No. 2010CB833004 and No. 2010CB832805.

- 
- [1] A. G. Riess *et al.* [Supernova Search Team Collaboration], *Astron. J.* **116**, 1009 (1998) [astro-ph/9805201].
  - [2] S. Perlmutter *et al.* [Supernova Cosmology Project Collaboration], *Astrophys. J.* **517**, 565 (1999) [astro-ph/9812133].
  - [3] V. Sahni, *Class. Quant. Grav.* **19**, 3435 (2002) [astro-ph/0202076].
  - [4] T. Padmanabhan, *Phys. Rept.* **380**, 235 (2003) [hep-th/0212290].
  - [5] N. Suzuki, D. Rubin, C. Lidman, G. Aldering, R. Amanullah, K. Barbary, L. F. Barrientos and J. Botyanszki *et al.*, *Astrophys. J.* **746**, 85 (2012) [arXiv:1105.3470 [astro-ph.CO]].
  - [6] G. Hinshaw *et al.* [WMAP Collaboration], *Astrophys. J. Suppl.* **208**, 19 (2013) [arXiv:1212.5226 [astro-ph.CO]].
  - [7] P. A. R. Ade *et al.* [Planck Collaboration], arXiv:1303.5076 [astro-ph.CO].
  - [8] A. G. Riess, L. Macri, S. Casertano, H. Lampeitl, H. C. Ferguson, A. V. Filippenko, S. W. Jha and W. Li *et al.*, *Astrophys. J.* **730**, 119 (2011) [Erratum-ibid. **732**, 129 (2011)] [arXiv:1103.2976 [astro-ph.CO]].

- [9] W. L. Freedman, B. F. Madore, V. Scowcroft, C. Burns, A. Monson, S. E. Persson, M. Seibert and J. Rigby, *Astrophys. J.* **758**, 24 (2012) [arXiv:1208.3281 [astro-ph.CO]].
- [10] J. -Q. Xia, H. Li and X. Zhang, *Phys. Rev. D* **88**, 063501 (2013) [arXiv:1308.0188 [astro-ph.CO]].
- [11] C. Cheng and Q. -G. Huang, *Phys. Rev. D* **89**, 043003 (2014) [arXiv:1306.4091 [astro-ph.CO]].
- [12] B. Hu, M. Liguori, N. Bartolo and S. Matarrese, *Phys. Rev. D* **88**, 123514 (2013) [arXiv:1307.5276 [astro-ph.CO]].
- [13] Z. Li, P. Wu, H. Yu and Z. -H. Zhu, *Sci. China Phys. Mech. Astron.* **57**, 381 (2014) [arXiv:1311.3467 [astro-ph.CO]].
- [14] G. Efstathiou, arXiv:1311.3461 [astro-ph.CO].
- [15] N. Suzuki *et al.*, *Astrophys. J.* **746**, 85 (2012) [arXiv:1105.3470 [astro-ph.CO]].
- [16] S. -N. Zhang and Y. -Z. Ma, arXiv:1303.6124 [astro-ph.CO].
- [17] J. Simon, L. Verde and R. Jimenez, *Phys. Rev. D* **71**, 123001 (2005) [astro-ph/0412269].
- [18] D. Stern, R. Jimenez, L. Verde, M. Kamionkowski and S. A. Stanford, *JCAP* **1002**, 008 (2010) [arXiv:0907.3149 [astro-ph.CO]].
- [19] M. Moresco, A. Cimatti, R. Jimenez, L. Pozzetti, G. Zamorani, M. Bolzonella, J. Dunlop and F. Lamareille *et al.*, *JCAP* **1208**, 006 (2012) [arXiv:1201.3609 [astro-ph.CO]].
- O. Farooq and B. Ratra, *Astrophys. J.* **766**, L7 (2013) [arXiv:1301.5243 [astro-ph.CO]].
- [20] G. Mangano, G. Miele, S. Pastor, T. Pinto, O. Pisanti and P. D. Serpico, *Nucl. Phys. B* **729**, 221 (2005) [hep-ph/0506164].
- [21] S. Nesseris and L. Perivolaropoulos, *Phys. Rev. D* **72**, 123519 (2005) [astro-ph/0511040].
- [22] F. Beutler, C. Blake, M. Colless, D. H. Jones, L. Staveley-Smith, L. Campbell, Q. Parker and W. Saunders *et al.*, *Mon. Not. Roy. Astron. Soc.* **416**, 3017 (2011) [arXiv:1106.3366 [astro-ph.CO]].
- [23] D. J. Eisenstein and W. Hu, *Astrophys. J.* **496**, 605 (1998) [astro-ph/9709112].
- [24] W. J. Percival *et al.* [SDSS Collaboration], *Mon. Not. Roy. Astron. Soc.* **401**, 2148 (2010) [arXiv:0907.1660 [astro-ph.CO]].
- [25] D. J. Eisenstein, H. -j. Seo, E. Sirko and D. Spergel, *Astrophys. J.* **664**, 675 (2007) [astro-ph/0604362].
- [26] N. Padmanabhan, X. Xu, D. J. Eisenstein, R. Scalzo, A. J. Cuesta, K. T. Mehta and E. Kazin, *Mon. Not. Roy. Astron. Soc.* **427**, no. 3, 2132 (2012) [arXiv:1202.0090 [astro-ph.CO]].

- [27] L. Anderson, E. Aubourg, S. Bailey, D. Bizyaev, M. Blanton, A. S. Bolton, J. Brinkmann and J. R. Brownstein *et al.*, *Mon. Not. Roy. Astron. Soc.* **427**, no. 4, 3435 (2013) [arXiv:1203.6594 [astro-ph.CO]].
- [28] C. Blake, E. Kazin, F. Beutler, T. Davis, D. Parkinson, S. Brough, M. Colless and C. Contreras *et al.*, *Mon. Not. Roy. Astron. Soc.* **418**, 1707 (2011) [arXiv:1108.2635 [astro-ph.CO]].
- [29] E. Gaztanaga, R. Miquel and E. Sanchez, *Phys. Rev. Lett.* **103**, 091302 (2009) [arXiv:0808.1921 [astro-ph]].
- [30] W. Hu and N. Sugiyama, *Astrophys. J.* **471**, 542 (1996) [astro-ph/9510117].
- [31] Y. Wang and S. Wang, *Phys. Rev. D* **88**, 043522 (2013) [arXiv:1304.4514 [astro-ph.CO]].
- [32] D. L. Shafer and D. Huterer, *Phys. Rev. D* **89**, 063510 (2014) [arXiv:1312.1688 [astro-ph.CO]].